Chemistry & Biology
Brief Communication

Target-Selective Phototherapy Using a Ligand-Based Photosensitizer for Type 2 Cannabinoid Receptor

Shaojuan Zhang,[1,2,6] Ningyang Jia,[1,3,6] Pin Shao,[1,6] Qin Tong,[4] Xiang-Qun Xie,[4] and Mingfeng Bai[1,5,*]
[1]Department of Radiology, University of Pittsburgh, 100 Technology Drive, Pittsburgh, PA 15219, USA
[2]Department of Diagnostic Radiology, First Hospital of Medical School, Xi'an Jiaotong University, 277 Yanta West Road, 710061 Xi'an, PRC
[3]Department of Radiology, Eastern Hepatobiliary Surgery Hospital, Second Military Medical University, 225 Changhai Road, 200438 Shanghai, PRC
[4]Department of Pharmaceutical Sciences, Computational Chemical Genomics Screening Center, School of Pharmacy and Drug Discovery Institute, University of Pittsburgh, Pittsburgh, PA 15213, USA
[5]University of Pittsburgh Cancer Institute, 5150 Centre Avenue, Pittsburgh, PA 15232, USA
[6]These authors contributed equally to this work
*Correspondence: baim@upmc.edu
http://dx.doi.org/10.1016/j.chembiol.2014.01.009

SUMMARY

Phototherapy is a powerful, noninvasive approach for cancer treatment, with several agents currently in clinical use. Despite the progress and promise, most current phototherapy agents have serious side effects as they can lead to damage to healthy tissue, even when the photosensitizers are fused to targeting molecules due to nonspecific light activation of the unbound photosensitizer. To overcome these limitations, we developed a phototherapy agent that combines a functional ligand and a near infrared phthalocyanine dye. Our target is type 2 cannabinoid receptor (CB2R), considered an attractive therapeutic target for phototherapy given it is overexpressed by many types of cancers that are located at a surface or can be reached by an endoscope. We show that our CB2R-targeted phototherapy agent, IR700DX-mbc94, is specific for CB2R and effective only when bound to the target receptor. Overall, this opens up the opportunity for development of an alternative treatment option for CB2R-positive cancers.

INTRODUCTION

The therapeutic value of light has been known for more than 3,000 years, and a systematic understanding of phototherapy has only been established over the past century (Dolmans et al., 2003; Tong and Kohane, 2012). Two types of phototherapy have been particularly well studied: photodynamic therapy (PDT) and photothermal therapy (PTT). As the conventional phototherapy, PDT destroys neoplastic lesions with reactive oxygen species (ROS), which are produced by using light of specific wavelengths to irradiate the PDT agents (Oleinick et al., 2002). The main classes of PDT agents include porphyrin derivatives, chlorins, porphycenes, and phthalocyaines (De Rosa and Bentley, 2000). PDT has now been clinically used as a noninvasive technique for cancer treatment, mainly in dermatology, ophthalmology, and gastroenterology. To date, several PDT agents have been approved by the FDA to treat cancer, such as Photofrin, Levulan, Metvix, and Foscan (Triesscheijn et al., 2006). PTT ablates tumors by converting photonic energy to heat instead of ROS (Jori and Spikes, 1990). By causing temperatures to rise, PTT leads to irreversible damage to cancer cells (Tong and Kohane, 2012).

Despite the advances in phototherapy techniques, PDT and PTT have significant limitations. Most existing PDT and PTT agents lack tumor selectivity; therefore, normal tissues can also be damaged, leading to considerable side effects (Mitsunaga et al., 2011; Tong and Kohane, 2012). Although targeting molecules, such as antibodies (Copland et al., 2004; Lukianova-Hleb et al., 2011), antibody fragments (Qian et al., 2008), receptor ligands (Chen et al., 2013), and peptides (Kim et al., 2011; Kumar et al., 2012) can be attached to photosensitizers for targeted delivery, unbound photosensitizers can still damage normal tissues upon light irradiation. As such, it is critical to develop highly target-selective phototherapy approaches.

Recently, Mitsunaga et al. (2011) described a highly target-selective phototherapy approach, photoimmunotherapy (PIT), which uses target-specific photosensitizers based on monoclonal antibodies coupled with a near infrared (NIR) phthalocyanine dye, IR700DX. Unlike conventional PIT technique (Goff et al., 1991; Mew et al., 1983), the new PIT agents reported by Mitsunaga et al. (2011) caused effective therapeutic effect only when they bound to target cancer cells while unbound sensitizers did not produce phototoxicity. Considering the high cost and long circulation time of antibodies (Olafsen and Wu, 2010), we set out to investigate whether target-selective phototherapy can be achieved using small photosensitizers based on receptor ligands.

Here, we report a type 2 cannabinoid receptor (CB_2R)-targeted phototherapy study using a phototherapy agent, IR700DX-mbc94. CB_2R is a transmembrane G protein-coupled receptor (GPCR) that was first cloned in 1993 (Munro et al., 1993). Under basal conditions, CB_2R is expressed mainly in immune cells while the expression in other types of cells is low to undetectable (Munro et al., 1993; Sexton et al., 2011). However, CB_2R is overexpressed by many types of cancers, such

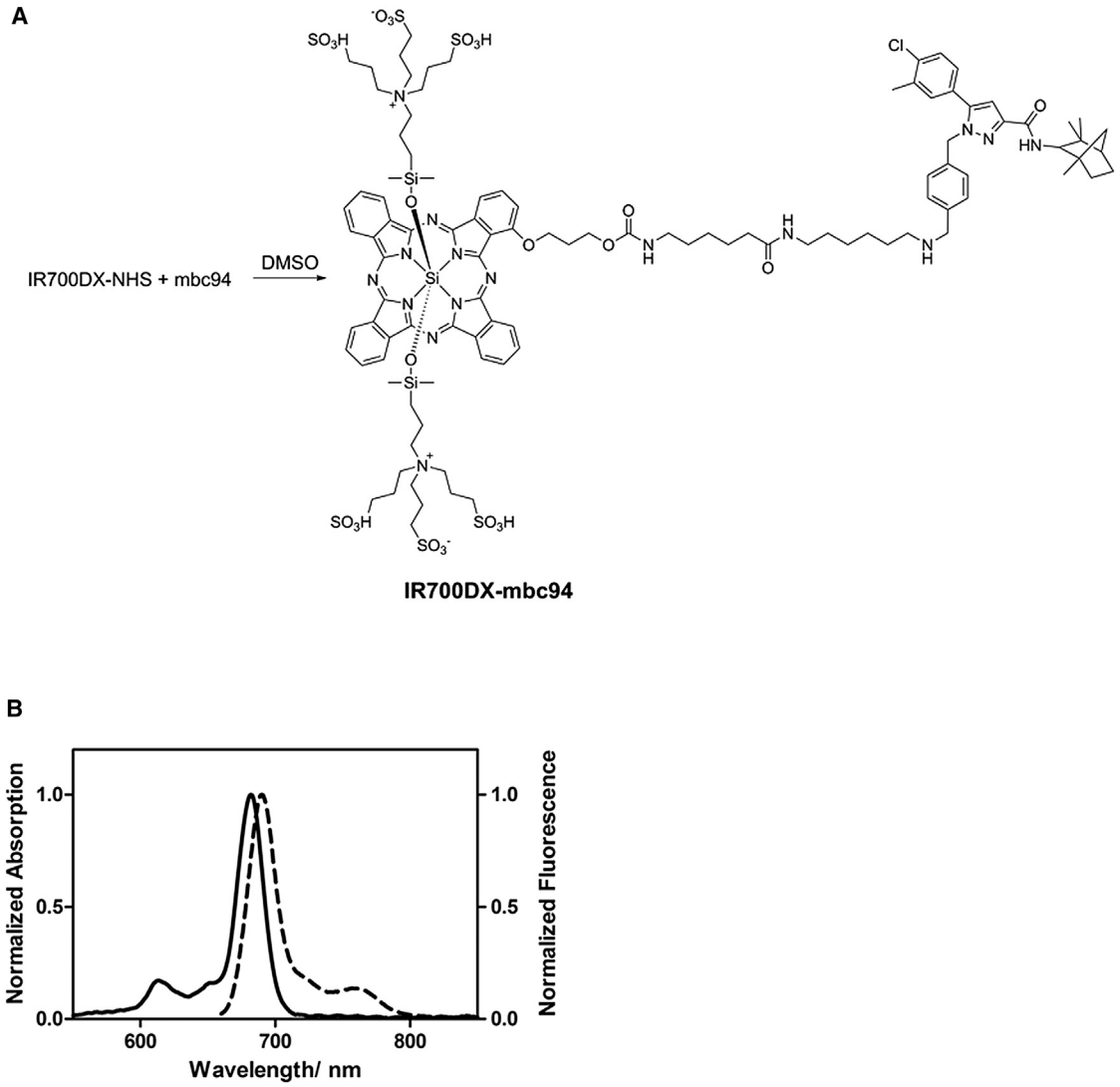

Figure 1. Synthesis and Photophysical Properties of IR700DX-mbc94

(A) Synthesis of IR700DX-mbc94.

(B) Absorption (solid) and emission (dotted) spectra of IR700DX-mbc94 in MeOH at a concentration of 1 μM (λex = 640 nm).

as prostate, skin, liver, and breast cancer, and moreover, the expression levels of CB_2R appear to be associated with tumor aggressiveness (Qamri et al., 2009; Velasco et al., 2012; Xu et al., 2006). Such upregulation of the receptor in cancer cells provides an opportunity to specifically target CB_2R and thus lower the side effects. Importantly, because many types of the CB_2R positive cancers are superficial or can be reached by endoscope, CB_2R has great potential as a phototherapy target. We previously reported an NIR CB_2R-targeted imaging probe, NIR-mbc94, and validated its specific binding to CB_2R in vitro (Bai et al., 2008; Sexton et al., 2011). More recently, we reported the CB_2R-targeted in vivo optical imaging using another NIR fluorescent probe, NIR760-mbc94 (Zhang et al., 2013). In this study, we developed IR700DX-mbc94 as the CB_2R receptor-targeted photosensitizer. We found that IR700DX-mbc94 caused significant cancer cell death only when bound to the target receptor. This photosensitizer appears to have great potential in cancer phototherapy with high target specificity.

RESULTS AND DISCUSSION

IR700DX-mbc94 was synthesized by coupling IR700DX with mbc94, a conjugable CB_2R ligand previously reported by us (Figure 1A) (Bai et al., 2008; Sexton et al., 2011). As displayed in Figure 1B, IR700DX-mbc94 exhibited an intense NIR absorption centered at 682 nm and maximum emission at 690 nm in methanol. The relatively small Stokes shift is typical for phthalocyanine dyes (Li et al., 2008).

To study the phototherapeutic effect of IR700DX-mbc94, we used CB_2-mid DBT cells, a transfected mouse malignant astrocytoma cell line that expresses CB_2R at the endogenous levels. Wild-type (WT) DBT cells that have no CB_2R expression were used as negative control (Cudaback et al., 2010).

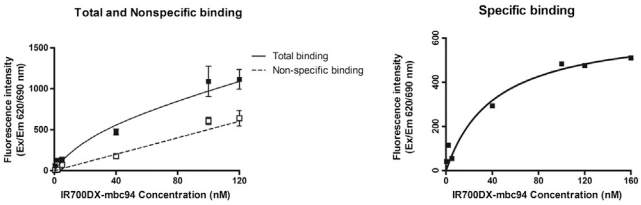

Figure 2. In Vitro CB_2R Saturation Binding Assay of IR700DX-mbc94

Cells were preincubated with (nonspecific binding) or without (total binding) 1 μM of the blocking agent SR144528 for 1 hr and then incubated overnight with an increasing concentration of IR700DX-mbc94 at 37°C. Cells were then rinsed and the fluorescence intensity was recorded. The specific binding was obtained by the subtraction of nonspecific binding from the total binding. The dissociation constant (K_D) and receptor density (Bmax) were estimated from the nonlinear fitting of specific binding versus IR700DX-mbc94 concentration using Prism software. Each data point represents the mean ± SD based on triplicate samples.

To measure the cytotoxicity of IR700DX-mbc94 in the absence of light irradiation in CB_2-mid DBT cells, we used the CellTiter-Glo Luminescent Cell Viability Assay kit. As shown in Figure S1A, available online, cells incubated with as high as 10 μM of IR700DX-mbc94 exhibited comparable low cytotoxicity to those treated with indocyanine green (ICG), the only Food and Drug Administration (FDA)-approved NIR fluorescent dye. We also found that the cytotoxic effect of IR700DX-mbc94 was significantly lower than that of mbc94 alone. The relatively high cytotoxicity of mbc94 was expected, as it had been reported that many CB_2R ligands exhibited anticancer properties (Velasco et al., 2012). It is possible that attaching IR700DX to mbc94 changed the binding profile of mbc94, leading to decreased CB_2R activation and therapeutic effect. In addition, to show the toxicity of IR700DX-mbc94 in noncancerous cells that express the CB_2R, we used CB_2R-transfected Chinese hamster ovarian (CHO-K1/CB2) cells (Gertsch et al., 2008). The cytotoxicity of IR700DX-mbc94 in CHO-K1/CB2 cells was as low as that in CB_2-mid DBT cells (Figure S1B). These combined data suggest that IR700DX-mbc94 is a safe agent in the absence of light irradiation.

To determine IR700DX-mbc94's binding affinity to CB_2R in intact cells, we used an in vitro saturation binding assay to measure the equilibrium dissociation constant (K_D) and the maximum specific binding (Bmax). A representative saturation binding curve is shown in Figure 2. From this data, we estimated that IR700DX-mbc94 bound to CB_2R with a K_D of 42.0 nM (±19.6) and Bmax of 650.5 pmol/mg (±93.1). Bmax over K_D value was ~15, indicating favorable binding for in vitro phototherapy experiments and future in vivo imaging studies.

We then carried out in vitro phototherapy experiments using IR700DX-mbc94 and light irradiation. CB_2-mid DBT cells were incubated with 5 μM of IR700DX-mbc94 at 37°C overnight. Cells were then washed twice and irradiated with light from a light-emitting diode (LED) light source at wavelengths of 670–710 nm (peak at 690 nm) and a power density of 30 mW/cm^2. As shown in Figure 3A, CB_2-mid DBT cells incubated with IR700DX-mbc94 did not show significant cell death (1.6% ± 1.4%) without light irradiation; however, irradiation of light for 20 min eradicated 79.5% ± 2.4% of the living cells. Similarly, there was little cell death associated with light irradiation in the absence of IR700DX-mbc94 (10.4% ± 2.0%). In addition, unbound IR700DX-mbc94 did not appear to contribute to the therapeutic effect, as we observed a similar level of cell death whether unbound IR700DX-mbc94 was washed (79.5% ± 2.4% cell death) or not (76.2% ± 5.3% cell death) (Figure 3B). We found that as much as 87.2% ± 2.0% of IR700DX-mbc94 was washed out (Figure 3C). To further investigate the target-specific phototherapy effect of IR700DX-mbc94, we compared phototoxicity between free IR700DX dye and IR700DX-mbc94. As expected, CB_2-mid DBT cells incubated with the same concentration of free IR700DX (5 μM) showed minimal cell death under light irradiation, whether the cells were washed (6.0% ± 4.5% cell death) or not (6.7% ± 3.7% cell death) (Figure 3D). We also studied the role of IR700DX-mbc94 binding in phototherapy by comparing the therapeutic effect on CB_2-mid and WT DBT cells. As shown in Figure 3E, WT-DBT cells treated with IR700DX-mbc94 followed by light irradiation showed significantly less cell death than CB_2-mid DBT cells (46.7% ± 7.9% versus 79.5% ± 2.4%, $p = 0.002$). This provides additional evidence that the ability of IR700DX-mbc94 to kill cancer cells required receptor binding. These combined data indicate that IR700DX-mbc94 causes cell death in a target-specific manner. Additionally, increased cell death was observed with an increased dose of light irradiation, higher concentration of IR700DX-mbc94 or longer incubation time (Figure S2). Furthermore, the potential of IR700DX-mbc94 for treating tumors in vivo was preliminarily assessed using a mouse tumor model. The experiments were approved by University of Pittsburgh Institutional Animal Care and Use Committee. CB_2-mid DBT cells were subcutaneously injected into mice to grow tumor. We found that tumor growth was significantly inhibited in the phototherapy-treated group using IR700DX-mbc94 compared with the nontreatment group (average tumor volume: 134.98 mm^3 in phototherapy-treated mice versus 780.16 mm^3 in untreated mice at day 7, $p = 0.03$) (Figure S3). This indicates that IR700DX-mbc94 has great potential as a phototherapy agent.

To study the mechanism underlying phototherapy of IR700DX-mbc94, we first investigated whether the therapeutic effect correlated with the generation of ROS, which trigger cell death during PDT. There are two types of PDT mechanisms: type I produces free radicals such as hydroxyl radicals (HO·), which can be inhibited by 1,3-dimethyl-2-thiourea (DMTU) (Sagone et al., 1989), and type II produces singlet oxygen ($^1O_2$) (Huang et al., 2012), which can be scavenged by sodium azide (NaN_3) (Mitsunaga et al., 2011). Studies have shown that DMTU could pass through cell membrane (Lai et al., 1999) and NaN_3 is an effective scavenger of intracellularly generated singlet oxygen (Sparrow et al., 2002). Therefore, although IR700DX-mbc94 is primarily located inside the cells as discussed below, DMTU and NaN_3 are effective ROS inhibitors. We found that treatment of CB_2-mid DBT cells with DMTU (1 mM) did not significantly affect the therapeutic effect of IR700DX-mbc94 under light irradiation (cell death 80.5% ± 7.6% with DMTU versus 79.4% ± 1.2% without DMTU, Figure 3F). In addition, the use of NaN_3 (50 mM) did not reverse the therapeutic effect either (cell death 87.1% ± 0.1% with

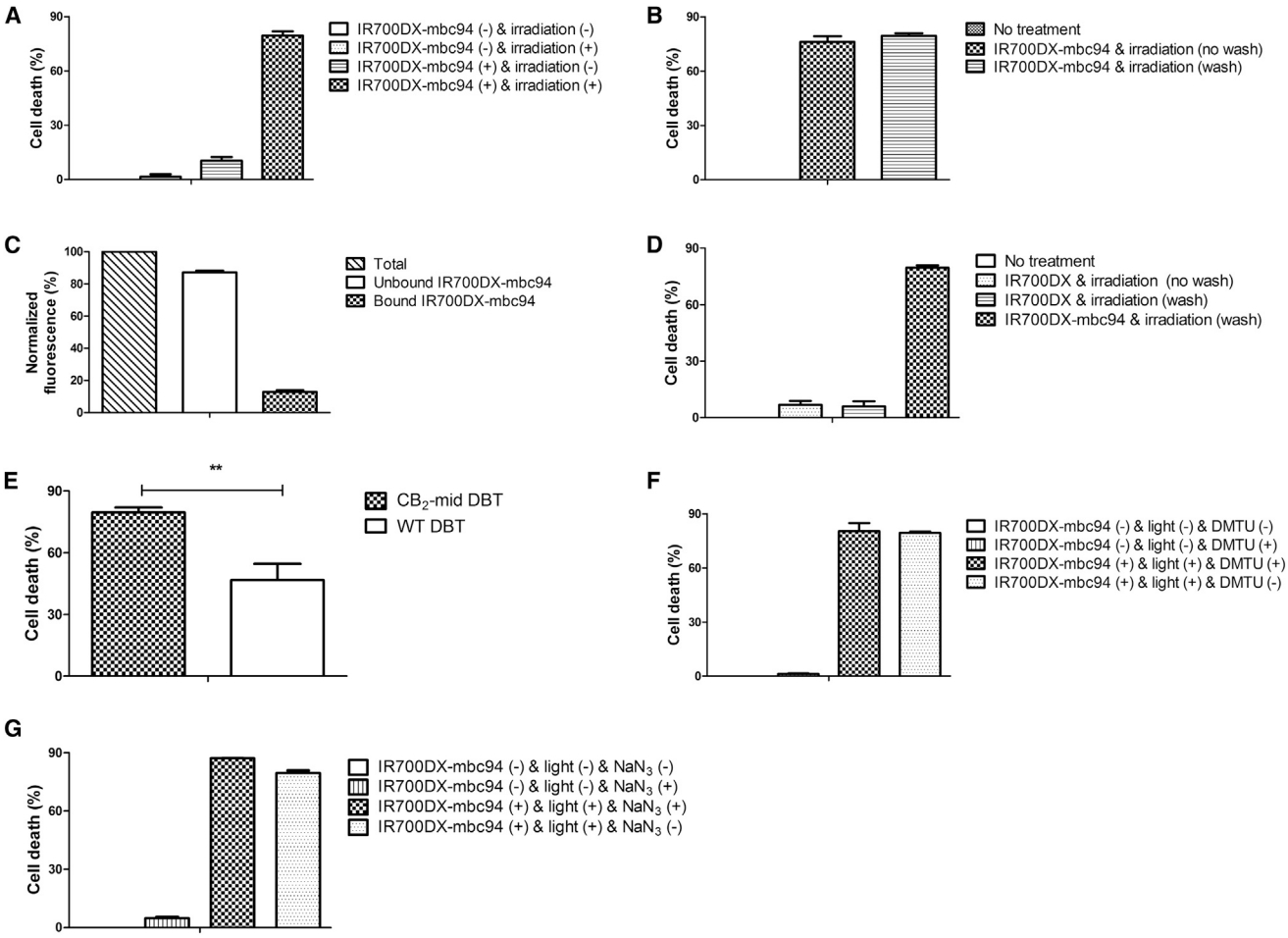

Figure 3. In Vitro Phototherapy Using IR700DX-mbc94

(A) Comparison of phototherapy effect on CB_2-mid DBT cells among four groups: IR700DX-mbc94 (−) and irradiation (−); IR700DX-mbc94 (−) and irradiation (+); IR700DX-mbc94 (+) and irradiation (−); and IR700DX-mbc94 (+) and irradiation (+).

(B) Phototherapy effect on CB_2-mid DBT cells incubated with 5 μM of IR700DX-mbc94 with or without wash.

(C) Quantification of unbound (photosensitizer that was washed out) and bound (remaining photosensitizer after washing) IR700DX-mbc94 using fluorescence.

(D) Phototherapy effect compared between CB_2-mid DBT cells treated with IR700DX-mbc94 (5 μM) and free IR700DX dye (5 μM).

(E) Comparison of cell death caused by IR700DX-mbc94 exposed to light irradiation between CB_2-mid DBT and WT-DBT cells (**$p < 0.01$).

(F) Effect of DMTU (1 mM) inhibition on cell death caused by IR700DX-mbc94 phototherapy.

(G) Effect of sodium azide (50 mM) inhibition on cell death caused by IR700DX-mbc94 phototherapy. Each data point represents the mean ± SD based on triplicate samples.

See also Figures S2 and S3.

NaN_3 versus 79.5% ± 2.4% without NaN_3, Figure 3G). Based on the above data, it appears that the phototherapeutic mechanism of IR700DX-mbc94 is distinct from the traditional PDT effect. However, further studies are needed to elucidate the mechanism of IR700DX-mbc94's therapeutic effect, which are beyond the scope of this study.

To visualize cell death caused by phototherapy of IR700DX-mbc94, CB_2-mid DBT cells were imaged under fluorescence microscopy with or without phototherapy (Figure 4). Cells treated with IR700DX-mbc94 in the absence of irradiation exhibited a normal morphology, and IR700DX-mbc94 was mainly located in the cytoplasm. In contrast, cells treated with IR700DX-mbc94 with light irradiation showed morphological changes typically observed in necrotic cell death, such as small blebs formation, cytoplasmic swelling, cell membrane rupture, and cell contents' release (Golstein and Kroemer, 2007). These morphological changes are similar to those previously reported for PIT, in which an IR700DX-conjugated monoclonal antibody was used as the PIT probe (Mitsunaga et al., 2011). To investigate whether internalization of IR700DX-mbc94 played an important role in the phototherapy effects, we used LysoTracker to find out if some IR700DX-mbc94 molecules were internalized and ended in lysosomal degradation. We observed certain colocalization (orange color) of LysoTracker and IR700DX-mbc94 fluorescence after 2 hr of incubation, indicating that part of IR700DX-mbc94 was internalized. In addition, IR700DX-mbc94 was shown to be primarily localized in the cytoplasm (Figures 4 and S4), which

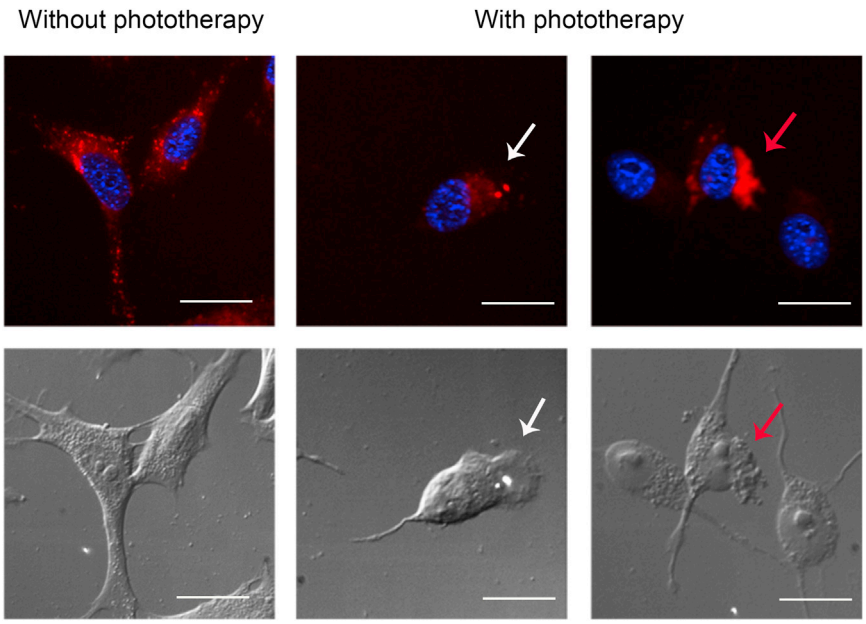

Figure 4. Fluorescence Microscopy of CB_2-Mid DBT Cells with or without Phototherapy

CB_2-mid DBT cells were treated with 5 μM of IR700DX-mbc94 at 37°C overnight, with or without light irradiation (30 mW/cm^2, 20 min). Upper panel: IR700DX-mbc94 (red fluorescence) and DAPI (blue fluorescence) images. Lower panel: differential interference contrast (DIC) images. With phototherapy treatment, cells experienced typical necrotic cell morphological changes, such as bleb formation (white arrowhead), cell membrane rupture and releasing of cells' contents (red arrowhead). Scale bar represents 20 μm.

See also Figure S4.

is consistent with recent studies reporting that CB_2R is primarily located at intracellular sites in certain cell lines (Castaneda et al., 2013). Based on these observations, it is likely that some IR700DX-mbc94 molecules bound to the surface CB_2R and internalized, whereas the majority of IR700DX-mbc94 molecules diffused into the cells and bound to intracellular CB_2R. We also noted that compared with IR700DX-based PIT (Mitsunaga et al., 2011), 10-fold of light was needed in CB_2R-targeted phototherapy to achieve similar therapeutic effects. This is likely due to the relatively low binding affinity of IR700DX-mbc94 to CB_2R compared with that of the antibody-antigen binding.

SIGNIFICANCE

We report a type 2 cannabinoid receptor-targeted phototherapy study using a photosensitizer (IR700DX-mbc94) based on a NIR phthalocyanine dye and a functional CB_2R-targeted molecule. IR700DX-mbc94 was only effective when bound to the target receptor and produced no phototoxicity when not bound, and the extent of the phototherapeutic effect of IR700DX-mbc94 was much less in CB_2R– than in CB_2R+ cells, suggesting a highly specific receptor-targeted phototherapy mechanism. Overall, receptor-targeted phototherapy provides a facile, target-specific approach based on small molecule photosensitizers with the advantages of low cost, easy delivery, and fast clearance. In addition, the discovery of receptor-targeted phototherapy may open opportunities to develop receptor targeted phototherapy techniques in general because various receptor ligands or peptides can be conjugated to IR700DX as potential phototherapy agents. Therefore, IR700DX-mbc94 appears to be an attractive phototherapy and therapeutic monitoring agent for the treatment of cancers.

EXPERIMENTAL PROCEDURES

Synthesis of IR700DX-mbc94

A mixture of IR700DX-NHS ester (2.5 mg, 1.28 μmol) and mbc94 (3 mg, 5.08 μmol) in DMSO (1 ml) was stirred at room temperature under argon for 24 hr in the absence of light. DMSO was removed by lyophilization, and the residue was washed by ethyl acetate (10 ml × 3) and dried by lyophilization.

In Vitro Saturation Binding Assay of IR700DX-mbc94

We carried out intact cell saturation binding assay to determine CB_2R binding affinity to IR700DX-mbc94 as previously reported (Zhang et al., 2013).

Cytotoxicity

CB_2-mid DBT cells were treated with indicated concentration of IR700DX-mbc94, or mbc94, without light irradiation for 24 hr in a water-jacketed incubator. ICG (Sigma-Aldrich) was used as the negative control and doxorubicin hydrochloride (Fisher Scientific) was used as the positive control. To test the toxicity of the IR700DX-mbc94 in cells that express the CB_2 receptor but are not tumoral, CHO-K1/CB2 cells were treated with indicated concentration of IR700DX-mbc94 for 24 hr. Cell viability was determined by CellTiter-Glo Luminescent Cell Viability Assay kit (Promega) according to the manufacturer's instructions.

In Vitro Phototherapy

CB_2-mid (CB_2R+) and WT (CB_2R−) DBT cells were grown to confluence in T75 flasks, harvested, seeded into 96-well optical plates, and incubated in a water-jacketed incubator for 24 hr prior to treatment. Each type of DBT cells was incubated with 5 μM of IR700DX-mbc94 at 37°C overnight. Cells were then irradiated with light from an LED light source (L690-66-60, Marubeni America) at wavelengths of 670–710 nm (peak at 690 nm) and a power density of 30 mW/cm^2, as measured with an optical power meter (PM100, Thorlabs). We compared the number of dead cells after the following treatments: IR700DX-mbc94 (−) and irradiation (−); IR700DX-mbc94 (−) and irradiation (+); IR700DX-mbc94 (+) and irradiation (−); and IR700DX-mbc94 (+) and irradiation (+). In addition, to investigate whether a higher amount of IR700DX-mbc94 in the surrounding medium will induce more cell death, we compared the phototherapy effect in cells that were washed and not washed. To quantify the unbound and bound IR700DX-mbc94, we measured the fluorescence intensities of the combined serum-free washing medium and the washed cells. Furthermore, we compared CB_2-mid DBT cells treated with free IR700DX dye (5 μM) with those treated with IR700DX-mbc94 (5 μM). The CB_2R-targeted phototherapy effect was then evaluated between CB_2-mid and WT DBT cells. To study whether the mechanism of phototherapy differs from that of PDT, a free radical scavenger DMTU (1 mM) or a $^1O_2$ quencher NaN_3 (50 mM) was added with IR700DX-mbc94 to CB_2-mid

DBT cells right before 20 min of light irradiation. We also tested whether the phototherapeutic effect is dependent on the dose of light irradiation, incubation time, and concentration of IR700DX-mbc94.

Fluorescent Microscopy

CB_2-mid DBT cells were incubated with 5 μM of IR700DX-mbc94 at 37°C overnight and then washed with fetal bovine serum (FBS)-free medium once. The cells were divided into two groups, with or without light irradiation (30 mW/cm^2, 20 min). Cell fluorescent staining was carried out as previously reported (Zhang et al., 2013). IR700DX-mbc94 fluorescent images were captured with a NIR camera equipped with a Cy5 filter set (excitation/emission: 625–655 nm/665–715 nm). Nuclear images were obtained with a DAPI filter set (excitation/emission: 335–383 nm/420–470 nm). Differential interference contrast (DIC) images were obtained through Trans light DIC.

SUPPLEMENTAL INFORMATION

Supplemental Information includes Supplemental Experimental Procedures and four figures and can be found with this article online at http://dx.doi.org/10.1016/j.chembiol.2014.01.009.

ACKNOWLEDGMENTS

We thank Dr. Nephi Stella at the University of Washington for providing DBT cells and technical advice. This work was supported by the startup fund provided by the Department of Radiology, University of Pittsburgh. This project used the UPCI imaging facilities supported, in part, by award P30CA047904. We also thank the Grant of Shanghai Science and Technology (12DZ1940606 and12ZR1439900) and Grant of Shanghai Municipal Health Bureau (20124195) for supporting N.J.'s work. We also thank the National Institutes of Health National Institute on Drug Abuse (NIH NIDA) for grant R01DA025612 (to X.-Q.X.).

Received: October 19, 2013
Revised: December 29, 2013
Accepted: January 23, 2014
Published: February 27, 2014

REFERENCES

Bai, M., Sexton, M., Stella, N., and Bornhop, D.J. (2008). MBC94, a conjugable ligand for cannabinoid CB 2 receptor imaging. Bioconjug. Chem. *19*, 988–992.

Castaneda, J.T., Harui, A., Kiertscher, S.M., Roth, J.D., and Roth, M.D. (2013). Differential expression of intracellular and extracellular CB(2) cannabinoid receptor protein by human peripheral blood leukocytes. J. Neuroimmune Pharmacol. *8*, 323–332.

Chen, Q., Li, K., Wen, S., Liu, H., Peng, C., Cai, H., Shen, M., Zhang, G., and Shi, X. (2013). Targeted CT/MR dual mode imaging of tumors using multifunctional dendrimer-entrapped gold nanoparticles. Biomaterials *34*, 5200–5209.

Copland, J.A., Eghtedari, M., Popov, V.L., Kotov, N., Mamedova, N., Motamedi, M., and Oraevsky, A.A. (2004). Bioconjugated gold nanoparticles as a molecular based contrast agent: implications for imaging of deep tumors using optoacoustic tomography. Mol. Imaging Biol. *6*, 341–349.

Cudaback, E., Marrs, W., Moeller, T., and Stella, N. (2010). The expression level of CB1 and CB2 receptors determines their efficacy at inducing apoptosis in astrocytomas. PLoS ONE *5*, e8702.

De Rosa, F.S., and Bentley, M.V. (2000). Photodynamic therapy of skin cancers: sensitizers, clinical studies and future directives. Pharm. Res. *17*, 1447–1455.

Dolmans, D.E., Fukumura, D., and Jain, R.K. (2003). Photodynamic therapy for cancer. Nat. Rev. Cancer *3*, 380–387.

Gertsch, J., Leonti, M., Raduner, S., Racz, I., Chen, J.Z., Xie, X.Q., Altmann, K.H., Karsak, M., and Zimmer, A. (2008). Beta-caryophyllene is a dietary cannabinoid. Proc. Natl. Acad. Sci. USA *105*, 9099–9104.

Goff, B.A., Bamberg, M., and Hasan, T. (1991). Photoimmunotherapy of human ovarian carcinoma cells ex vivo. Cancer Res. *51*, 4762–4767.

Golstein, P., and Kroemer, G. (2007). Cell death by necrosis: towards a molecular definition. Trends Biochem. Sci. *32*, 37–43.

Huang, L., Xuan, Y., Koide, Y., Zhiyentayev, T., Tanaka, M., and Hamblin, M.R. (2012). Type I and Type II mechanisms of antimicrobial photodynamic therapy: an in vitro study on gram-negative and gram-positive bacteria. Lasers Surg. Med. *44*, 490–499.

Jori, G., and Spikes, J.D. (1990). Photothermal sensitizers: possible use in tumor therapy. J. Photochem. Photobiol. B *6*, 93–101.

Kim, Y.H., Jeon, J., Hong, S.H., Rhim, W.K., Lee, Y.S., Youn, H., Chung, J.K., Lee, M.C., Lee, D.S., Kang, K.W., and Nam, J.M. (2011). Tumor targeting and imaging using cyclic RGD-PEGylated gold nanoparticle probes with directly conjugated iodine-125. Small *7*, 2052–2060.

Kumar, A., Ma, H., Zhang, X., Huang, K., Jin, S., Liu, J., Wei, T., Cao, W., Zou, G., and Liang, X.J. (2012). Gold nanoparticles functionalized with therapeutic and targeted peptides for cancer treatment. Biomaterials *33*, 1180–1189.

Lai, Y.L., Chiou, W.Y., Lu, F.J., and Chiang, L.Y. (1999). Roles of oxygen radicals and elastase in citric acid-induced airway constriction of guinea-pigs. Br. J. Pharmacol. *126*, 778–784.

Li, Y.J., Pritchett, T.M., Huang, J.D., Ke, M.R., Shao, P., and Sun, W.F. (2008). Photophysics and nonlinear absorption of peripheral-substituted zinc phthalocyanines. J. Phys. Chem. A *112*, 7200–7207.

Lukianova-Hleb, E.Y., Oginsky, A.O., Samaniego, A.P., Shenefelt, D.L., Wagner, D.S., Hafner, J.H., Farach-Carson, M.C., and Lapotko, D.O. (2011). Tunable plasmonic nanoprobes for theranostics of prostate cancer. Theranostics *1*, 3–17.

Mew, D., Wat, C.K., Towers, G.H., and Levy, J.G. (1983). Photoimmunotherapy: treatment of animal tumors with tumor-specific monoclonal antibody-hematoporphyrin conjugates. J. Immunol. *130*, 1473–1477.

Mitsunaga, M., Ogawa, M., Kosaka, N., Rosenblum, L.T., Choyke, P.L., and Kobayashi, H. (2011). Cancer cell-selective in vivo near infrared photoimmunotherapy targeting specific membrane molecules. Nat. Med. *17*, 1685–1691.

Munro, S., Thomas, K.L., and Abu-Shaar, M. (1993). Molecular characterization of a peripheral receptor for cannabinoids. Nature *365*, 61–65.

Olafsen, T., and Wu, A.M. (2010). Antibody vectors for imaging. Semin. Nucl. Med. *40*, 167–181.

Oleinick, N.L., Morris, R.L., and Belichenko, I. (2002). The role of apoptosis in response to photodynamic therapy: what, where, why, and how. Photochem. Photobiol. Sci. *1*, 1–21.

Qamri, Z., Preet, A., Nasser, M.W., Bass, C.E., Leone, G., Barsky, S.H., and Ganju, R.K. (2009). Synthetic cannabinoid receptor agonists inhibit tumor growth and metastasis of breast cancer. Mol. Cancer Ther. *8*, 3117–3129.

Qian, X., Peng, X.H., Ansari, D.O., Yin-Goen, Q., Chen, G.Z., Shin, D.M., Yang, L., Young, A.N., Wang, M.D., and Nie, S. (2008). In vivo tumor targeting and spectroscopic detection with surface-enhanced Raman nanoparticle tags. Nat. Biotechnol. *26*, 83–90.

Sagone, A.L., Jr., Husney, R.M., Wewers, M.D., Herzyk, D.J., and Davis, W.B. (1989). Effect of dimethylthiourea on the neutrophil myeloperoxidase pathway. J Appl Physiol *67*, 1056–1062.

Sexton, M., Woodruff, G., Horne, E.A., Lin, Y.H., Muccioli, G.G., Bai, M., Stern, E., Bornhop, D.J., and Stella, N. (2011). NIR-mbc94, a fluorescent ligand that binds to endogenous CB(2) receptors and is amenable to high-throughput screening. Chem. Biol. *18*, 563–568.

Sparrow, J.R., Zhou, J., Ben-Shabat, S., Vollmer, H., Itagaki, Y., and Nakanishi, K. (2002). Involvement of oxidative mechanisms in blue-light-induced damage to A2E-laden RPE. Invest. Ophthalmol. Vis. Sci. *43*, 1222–1227.

Tong, R., and Kohane, D.S. (2012). Shedding light on nanomedicine. Wiley Interdiscip. Rev. Nanomed. Nanobiotechnol. *4*, 638–662.

Triesscheijn, M., Baas, P., Schellens, J.H., and Stewart, F.A. (2006). Photodynamic therapy in oncology. Oncologist *11*, 1034–1044.

Velasco, G., Sánchez, C., and Guzmán, M. (2012). Towards the use of cannabinoids as antitumour agents. Nat. Rev. Cancer *12*, 436–444.

Xu, X., Liu, Y., Huang, S., Liu, G., Xie, C., Zhou, J., Fan, W., Li, Q., Wang, Q., Zhong, D., and Miao, X. (2006). Overexpression of cannabinoid receptors CB1 and CB2 correlates with improved prognosis of patients with hepatocellular carcinoma. Cancer Genet. Cytogenet. *171*, 31–38.

Zhang, S., Shao, P., and Bai, M. (2013). In vivo type 2 cannabinoid receptor-targeted tumor optical imaging using a near infrared fluorescent probe. Bioconjug. Chem. *24*, 1907–1916.

